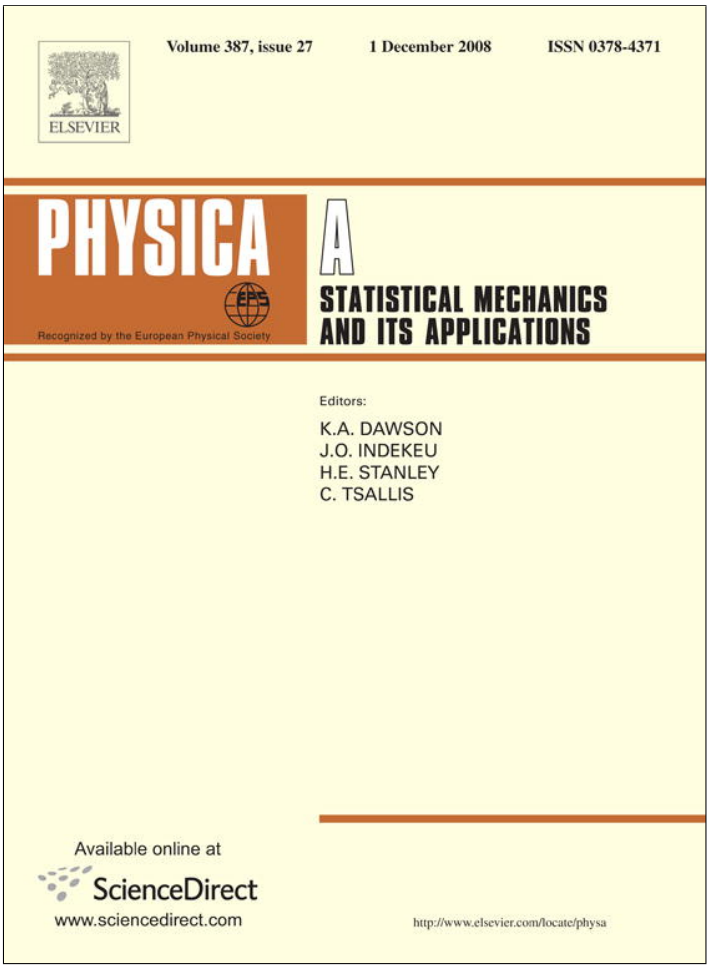

Physica A 387 (2008) 6705–6711

Contents lists available at ScienceDirect

Physica A

journal homepage: www.elsevier.com/locate/physa

Periodic boundary conditions and the correct molecular-dynamics ensemble

J.A. White [a,*], F.L. Román [a,b], A. González [a], S. Velasco [a]

[a] Departamento de Física Aplicada, Universidad de Salamanca, E-37008 Salamanca, Spain

[b] Escuela Politécnica Superior de Zamora, Universidad de Salamanca, E-49022 Zamora, Spain

ARTICLE INFO

Article history:
Received 11 June 2008
Received in revised form 26 July 2008
Available online 8 August 2008

PACS:
05.20.Gg
05.20.Jj

Keywords:
Periodic boundary conditions
Molecular-dynamics ensemble
Hard-disk fluid
Microscopic structure

ABSTRACT

The use of periodic boundary conditions in molecular-dynamics simulations leads to the microcanonical *EVN***MG** ensemble of Ray and Zhang [J.R. Ray, H. Zhang, Phys. Rev. E 59 (1999) 4781] in which the total linear momentum **M** and the generator of infinitesimal Galilean boosts **G** are conserved quantities in addition to the total energy E, the volume V, and the number of particles N of the system. We find that the invariance of **G** should be of importance in the analysis of ensemble averages of quantities that only depend on the spatial coordinate **r**. As an application we study the density profile of an isolated system of hard disks with periodic boundary conditions in the absence of external forces. We find that the periodic boundary conditions give rise to an anomalous inhomogeneity in the density profile of the system. This inhomogeneity is only relevant for systems with a very small number of disks and is related to the conservation of the center of mass coordinates.

1. Introduction

Let us consider a d-dimensional system with a finite number of particles N in a region of volume V, with constant total energy E. The equilibrium statistical-mechanics description of such a system is provided by the microcanonical (or *EVN*) ensemble in which E, V, and N are the only conserved quantities, i.e., these quantities are invariant under the evolution in the time t of the system. In the absence of external fields, a MD simulation of this system involves the use of periodic boundary conditions and therefore the total linear momentum **M** of the system is also conserved. In this case one has to deal with a special microcanonical ensemble: the *EVN***M** or Molecular-Dynamics ensemble [1–3]. Until recently, this ensemble has been considered the appropriate framework for MD simulations [1–4,7,8,5,6]. However, in 1999 Ray and Zhang [9] realized that MD simulations also imply the conservation of the generator of infinitesimal Galilean boosts **G**, and thus the ensemble generated by MD simulations is really the *EVN***MG** ensemble. **G** is defined as [9]

$$\mathbf{G} = \sum_{i=1}^{N} \mathbf{p}_i t - \sum_{i=1}^{N} m_i \mathbf{r}_i \tag{1}$$

where $\mathbf{r}_i$, $\mathbf{p}_i$, and m_i correspond, respectively, to the position, the momentum, and the mass of particle i. As discussed by Ray and Zhang [9], **G** arises from integration of the constant total linear momentum

$$\mathbf{M} \equiv \sum_{i=1}^{N} \mathbf{p}_i = \sum_{i=1}^{N} m_i \frac{\mathrm{d}\mathbf{r}_i(t)}{\mathrm{d}t}, \tag{2}$$

* Corresponding author. Tel.: +34 923294436; fax: +34 923294584.
E-mail address: white@usal.es (J.A. White).

0378-4371/$ – see front matter © 2008 Elsevier B.V. All rights reserved.
doi:10.1016/j.physa.2008.08.008

and is associated with the initial position of the center of mass (CM) of the system. In 2000, Wood et al. [10] expressed their agreement with the invariance of **G** provided that the particle positions $\mathbf{r}_i$'s in Eq. (1) were defined as the *infinite-checkerboard* positions [3,2] instead of the simulation-cell positions. This avoids the discontinuity that arises in the particle position when a particle crosses the simulation-cell boundary to re-enter through the opposite face which in turn would imply that the d-dimensional vector **G** is not constant. Furthermore, Wood et al. [10] found it preferable to reformulate the time invariance of **G** in terms of a parameter **R** proportional to the CM of the system. Instead of using the Wood et al. [10] definition of **R**, for simplicity, here we denote by **R** the CM position itself, i.e.,

$$\mathbf{R} \equiv \frac{1}{M_{\text{tot}}} \sum_{i=1}^{N} m_i \mathbf{r}_i, \tag{3}$$

where $M_{\text{tot}} \equiv \sum_{i=1}^{N} m_i$ is the total mass of the system. A slightly different formulation of **G** was presented by Shirts et al. [11] by dividing this quantity by M_{tot} and incorporating a repeating-cell lattice vector $\boldsymbol{\sigma}_i$ that defines the cell to which the ith particle has moved in time t.

Ray and Zhang obtained for the *EVN***MG** ensemble the following probability density in phase space [9]

$$W_{EVN\mathbf{MG}}(\mathbf{r}^N, \mathbf{p}^N) = C\delta\left(E - H(\mathbf{r}^N, \mathbf{p}^N)\right) \delta\left(\mathbf{M} - \sum_{i=1}^{N} \mathbf{p}_i\right) \delta\left(\mathbf{G} - \sum_{i=1}^{N} \mathbf{p}_i t + \sum_{i=1}^{N} m_i \mathbf{r}_i\right) \tag{4}$$

where $(\mathbf{r}^N, \mathbf{p}^N) \equiv (\mathbf{r}_1, \ldots, \mathbf{r}_N, \mathbf{p}_1, \ldots, \mathbf{p}_N)$ are the phase coordinates of the system, $\delta(x)$ is the Dirac delta function, $H(\mathbf{r}^N, \mathbf{p}^N) = \sum_{i=1}^{N} \mathbf{p}_i^2/2m_i + U(\mathbf{r}^N)$ is the Hamiltonian of the system, and C is a normalization constant. The use of the Wood et al. [10] prescription would yield an equivalent expression for the probability density in phase space but replacing the δ function involving **G** in Eq. (4) by $\delta(\mathbf{R} - \sum_{i=1}^{N} m_i \mathbf{r}_i/M_{\text{tot}})$. A similar procedure would yield the result obtained by Shirts et al. [11] for $W_{EVN\mathbf{MG}}$.

All of the mentioned prescriptions for the *EVN***MG** ensemble are based on the same physical grounds, namely the conservation of E, V, N, **M**, and **G** (or, equivalently, **R**). While the treatment of the first four constraints is well established, the above discussion shows that the treatment of the **G** (**R**) constraint is not unique and leads to a different probability density W. This fact is not relevant if the probability density is used to obtain the average values of a quantity that only depends on momentum coordinates [11] and/or internal spatial coordinates [9,10] since in these situations the δ function involving the CM coordinates can be integrated out, reducing the number of spatial integrations by d and yielding the same results for the three considered prescriptions [9–11].

The goal of the present paper is to study the ensemble average $\langle A(\mathbf{r})\rangle$ of a quantity A that only depends on the spatial coordinate **r**. This study will allow us to gain further insight into the **G** constraint of the *EVN***MG** ensemble. As an application we shall analyze the one-particle density $\rho(\mathbf{r})$ of a system of hard disks with periodic boundary conditions. It is well-known that this system presents anomalous or implicit finite-size effects due to the periodic boundary conditions that induce an anisotropy in the pair correlation function [12–15] while the one-particle density is assumed to be constant. In this paper we shall show that the conservation of **M** and **G** associated with the periodic boundary conditions also gives rise to an anomalous inhomogeneity in the fluid, i.e., the one-particle density is no longer a constant quantity. The paper is structured as follows. In Section 2 an expression is obtained for $\langle A(\mathbf{r})\rangle$ in terms of *Mayer f-functions* and CM constraints. In Section 3 we compare our MD simulation results for the one-particle density with the predictions of the theory for $N = 2$ and 3 hard disks in the *EVN***MG** ensemble. We conclude with a summary of the main results of the present work.

2. Theory

The *EVN***MG** ensemble average of a quantity $A(\mathbf{r})$ is obtained from the following expression

$$\langle A(\mathbf{r})\rangle = \int A(\mathbf{r}) W_{EVN\mathbf{MG}}(\mathbf{r}^N, \mathbf{p}^N)\, \mathrm{d}\mathbf{r}^N\, \mathrm{d}\mathbf{p}^N. \tag{5}$$

Since $A(\mathbf{r})$ only depends on position coordinates, using Eq. (4) we can integrate out the momentum variables in Eq. (5) to obtain

$$\langle A(\mathbf{r})\rangle = \bar{C} \int \mathrm{d}\mathbf{r}^N A(\mathbf{r}) \left(E - \frac{\mathbf{M}^2}{2M_{\text{tot}}} - U(\mathbf{r}^N)\right)^{d(N-1)/2-1} \Theta\left(E - \frac{\mathbf{M}^2}{2M_{\text{tot}}} - U(\mathbf{r}^N)\right) \delta\left(\mathbf{G} - \mathbf{M}t + \sum_{i=1}^{N} m_i \mathbf{r}_i\right) \tag{6}$$

where $\Theta(x)$ is the Heaviside step function, $\bar{C}$ is a normalization constant, and the integrations leading to Eq. (6) have been carried out by resorting to Jacobi momentum variables [9] and using Laplace transform methods (see, e.g., Refs. [7,16]).

For hard particles, the integrand in (6) is non-vanishing only when the interparticle potential $U(\mathbf{r}^N)$ is equal to 0, i.e., when the particles in the system do not overlap. Therefore, for a system of hard particles with diameter σ, Eq. (6) can be rewritten as

$$\langle A(\mathbf{r})\rangle = \bar{C}\left(E-\frac{\mathbf{M}^2}{2M_{\rm tot}}\right)^{d(N-1)/2-1}\Theta\left(E-\frac{\mathbf{M}^2}{2M_{\rm tot}}\right)\int d\mathbf{r}^N A(\mathbf{r})\prod_{i<j}^{N}[1+f(|\mathbf{r}_i-\mathbf{r}_j|)]$$
$$\times\delta\left(\mathbf{G}-\mathbf{M}t+\sum_{i=1}^{N}m_i\mathbf{r}_i\right) \tag{7}$$

where $f(r) = -1$ for $r < \sigma$ and $f(r) = 0$ for $r > \sigma$, i.e., $f(r)$ corresponds to the *Mayer f-function* of a hard-particle interaction.

For simplicity we assume an inertial frame for which $\mathbf{M} = 0$ and $\mathbf{G} = -M_{\rm tot}\mathbf{R}$. In this case Eq. (7) becomes

$$\langle A(\mathbf{r})\rangle = \bar{\bar{C}}\int d\mathbf{r}^N A(\mathbf{r})\prod_{i<j}^{N}[1+f(|\mathbf{r}_i-\mathbf{r}_j|)]\delta\left(\mathbf{R}-\frac{1}{M_{\rm tot}}\sum_{i=1}^{N}m_i\mathbf{r}_i\right) \tag{8}$$

where $\bar{\bar{C}} = \bar{C}E^{d(N-1)/2-1}/M_{\rm tot}$.

As commented above (see also Ref. [10]), the constant-**G** (**R**) constraint in Eqs. (6)–(8) is based on assuming *infinite-checkerboard* positions [3,2] instead of simulation-cell positions (the MD coordinates). Therefore, in order to compare the results of Eq. (7) with MD data this constraint should be reinterpreted in terms of these coordinates. For simplicity let us consider a two-dimensional simulation cell ($d = 2$) with dimensions L_x, L_y, if the ith particle crosses the simulation-cell boundary located at $x = 0$ to re-enter through the opposite face located at $x = L_x$ one has $R_{x,new} = R_{x,old} + m_i L_x/M_{\rm tot}$, where R_x is the x coordinate of the CM position **R**. This scheme applies whenever a particle crosses a boundary (X or Y) and therefore **R** changes discontinuously to a new value in the simulation cell. At this point it is important to realize that if all particle masses are equal there are only N^d different, discrete locations for the CM position, and these locations are equally distributed in a rectangular sublattice with periodicity L_x/N, L_y/N, showing a lack of ergodicity in the system. The situation becomes more complicated for different masses. For rational mass ratios m_i/m_j, the CM positions still belong to a discrete set, but the periodicity of the underlying sublattice changes to L_x/N', L_y/N' where $N' = M_{\rm tot}/\gcd(m_1,\ldots,m_N)$, thus becoming more densely distributed. For irrational mass ratios the situation is even worse: since $N' \to \infty$, the CM positions are no longer discretely distributed in the simulation cell and one has to deal with a continuum distribution of CM positions.

In this paper we shall consider the simplest case for which all particles have equal mass ($m_i = m$ and $M_{\rm tot} = Nm$) and the CM positions are distributed in a discrete sublattice. In this situation the CM coordinates can only take the values

$$\mathbf{R}_{\alpha,\beta} = \left(R_{x,0}+\alpha\frac{L_x}{N}, R_{y,0}+\beta\frac{L_y}{N}\right) \tag{9}$$

where $R_{x,0}$ and $R_{y,0}$ denote the smallest values of the CM coordinates in the simulation cell and $0 \le \alpha, \beta \le N-1$. Since we have obtained a discrete set of values $\mathbf{R}_{\alpha,\beta}$ for the CM position, it seems natural to replace the δ function involving **R** in Eq. (8) by a sum of δ contributions involving the $\mathbf{R}_{\alpha,\beta}$'s defined in Eq. (9), i.e.,

$$\langle A(\mathbf{r})\rangle_{\rm pbc} = \bar{\bar{C}}\int d\mathbf{r}^N A(\mathbf{r})\prod_{i<j}^{N}[1+f(|\mathbf{r}_i-\mathbf{r}_j|_{\rm pbc})]\prod_{k=1}^{N}H(\mathbf{r}_k)\sum_{\alpha,\beta=0}^{N-1}\delta\left(\mathbf{R}_{\alpha,\beta}-\frac{1}{N}\sum_{i=1}^{N}\mathbf{r}_i\right) \tag{10}$$

where $H(\mathbf{r}_k)$ is a function that ensures that the region of integration for the kth particle is restricted to the simulation cell (it takes the value of 1 inside the cell and 0 otherwise). The label 'pbc' in Eq. (10) denotes that the distance between particles is measured taking into account the *actual* distance for simulation-cell positions in a system with periodic boundary conditions, namely

$$|\mathbf{r}_i-\mathbf{r}_j|_{\rm pbc} = \left(\mathrm{Min}\left[(x_i-x_j)^2,(L_x-|x_i-x_j|)^2\right]+\mathrm{Min}\left[(y_i-y_j)^2,(L_y-|y_i-y_j|)^2\right]\right)^{1/2}. \tag{11}$$

Eq. (10) is our final result for the *EVN***MG** ensemble average of $A(\mathbf{r})$ in a fluid of N hard disks with equal mass and subjected to periodic boundary conditions. This result should be compared with Eq. (8) which is valid for *infinite-checkerboard* positions. Three main differences arise between both results: (i) Eq. (8) only considers one CM position instead of the discrete set of CM positions of Eq. (10), (ii) the definition of distance in Eq. (10) is adapted to periodic boundary conditions and thus differs from the usual definition of distance considered in Eq. (8), and (iii) we have included a function $H(\mathbf{r})$ that accounts for the geometry of the simulation cell. The validity of Eq. (10) will be tested against MD results in Section 3.

Finally we would like to note that the sum of δ terms over lattice sites obtained for a system of hard disks with equal masses in Eqs. (10) and (13) can be straightforwardly extended to one or three dimensions and particles with different masses. For systems with irrational mass ratios, the sum over lattice sites should be replaced by an integral over **R**. Carrying out this integration would suppress the **R**-dependence of the ensemble averages in (10) and (13) and therefore, in this case, the effect of the CM constraint would be suppressed. This is what one observes, for instance, for a system with two disks with masses m and $\sqrt{2}m$ that presents an uniform density profile (not shown), in contrast with the inhomogeneous density profile of a system with two disks with equal masses considered in Section 3 [see Fig. 1(a)].

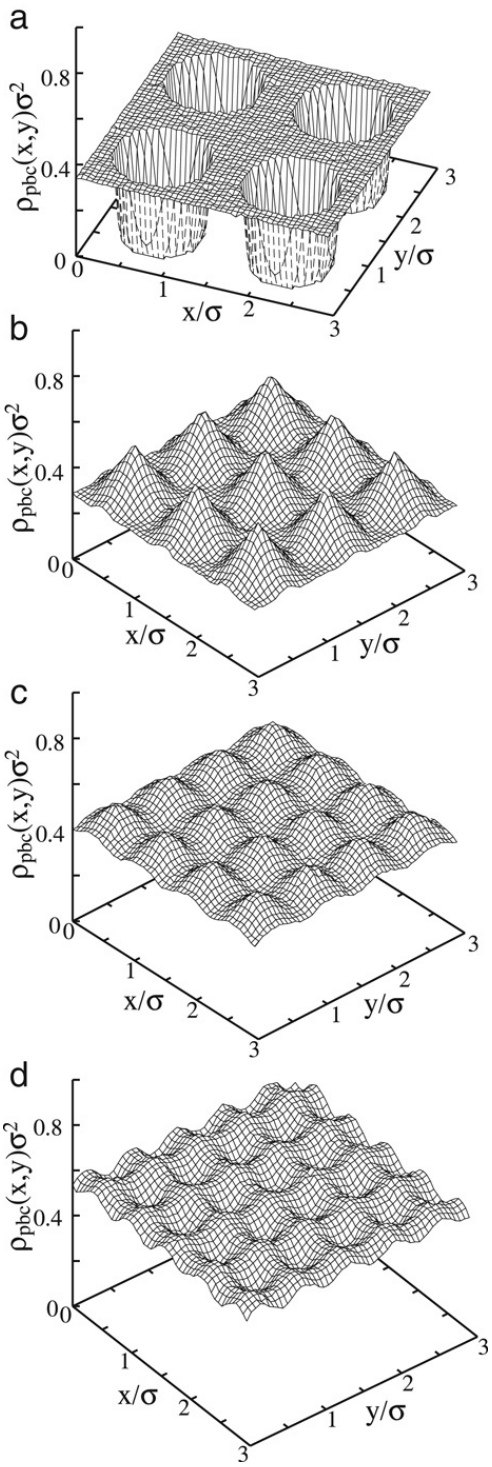

Fig. 1. Molecular-dynamics results for the density profile of a hard-disk fluid with periodic boundary conditions and different numbers of particles. In all cases $L_x = L_y = 3\sigma$; (a) $N = 2$, (b) $N = 3$, (c) $N = 4$, and (d) $N = 5$.

3. An example: The one-particle density

The one-particle density or density profile $\rho(\mathbf{r})$ of a fluid is defined as the ensemble average of the microscopic density

$$\hat{\rho}(\mathbf{r}) = \sum_{i=1}^{N} \delta(\mathbf{r}_i - \mathbf{r}), \tag{12}$$

and therefore, from Eq. (10), the density profile in the *EVN***MG** ensemble becomes

$$\rho_{\rm pbc}(\mathbf{r}) \equiv \langle \hat{\rho}(\mathbf{r}) \rangle_{\rm pbc} = \bar{\bar{C}} \int d\mathbf{r}^N \hat{\rho}(\mathbf{r}) \prod_{i<j}^{N} [1 + f(|\mathbf{r}_i - \mathbf{r}_j|_{\rm pbc})] \prod_{k=1}^{N} H(\mathbf{r}_k) \sum_{\alpha,\beta=0}^{N-1} \delta \left(\mathbf{R}_{\alpha,\beta} - \frac{1}{N} \sum_{i=1}^{N} \mathbf{r}_i \right). \tag{13}$$

This should be compared with the result for the density profile in the standard microcanonical *EVN* ensemble (or in the *EVN***M** ensemble) where one has

$$\rho_{{\rm pbc},EVN(\mathbf{M})} = \bar{\bar{C}} \int d\mathbf{r}^N \hat{\rho}(\mathbf{r}) \prod_{i<j}^{N} [1 + f(|\mathbf{r}_i - \mathbf{r}_j|_{\rm pbc})] \prod_{k=1}^{N} H(\mathbf{r}_k). \tag{14}$$

In this case, from Eq. (12), it is easy to realize that the density $\rho_{{\rm pbc},EVN(\mathbf{M})}$ is a constant quantity, i.e., the fluid is uniform, in contrast with the *EVN***MG** result (13) where the **G** constraint leads to an anomalous inhomogeneous density profile $\rho_{\rm pbc}(\mathbf{r})$.

In order to test the inhomogeneity of the density in the *EVN***MG** ensemble we have performed MD simulations for a hard-disk fluid with periodic boundary conditions, measuring the one-particle density in cases with a very reduced number of particles where we expect large deviations from the uniform fluid. In Fig. 1 we present our MD results for a fluid of $N = 2, 3, 4$, and 5 hard disks of diameter σ and mass m. The calculations have been performed in a simulation cell with $L_x = L_y = 3\sigma$ and using periodic boundary conditions. An event driven MD algorithm has been used in the simulations of the hard-disk system (see, e.g., Ref. [17] for details). Prior to starting the measurements, for each simulation we have considered an equilibration period of 10^5 collisions per particle. Then we have considered a measurement period of 3.5×10^6 collisions per particle. During this period we have performed 10^7 measurements of the density profile. Finally we would like to mention that the initial velocities of the disks have been chosen at random but fulfilling the constraint $\mathbf{M} = 0$.

In all cases presented in Fig. 1 it is observed that the fluid is indeed inhomogeneous with a density profile that presents a periodic structure in a square sublattice with N^2 cells. It seems evident that this structure is connected to the distribution of CM positions considered in Eq. (13). For instance, the initial value of the CM position for the $N = 2$ simulation was $(0.75\sigma, 0.75\sigma)$ which coincides with the center of one of the *holes* of radius $\sigma/2$ of the density profile [see Fig. 1(a)], the other *holes* are centered at the remaining sublattice sites—it is clear that for $N = 2$ disks the location of each CM will be the center of a excluded zone with radius $\sigma/2$. As an aside we note that a simulation with total linear momentum $\mathbf{M} \neq 0$ (not shown) yields a density profile with *stripes* (rather than holes) along the direction of **M**, due to the drift of the center of mass. For a larger number of disks the situation is similar but without excluded zones. In particular, the initial value of the CM position for the $N = 3$ simulation was $(0.5\sigma, 0.5\sigma)$ which coincides with the location of one of the peaks of the profile and the other peaks are located at the remaining lattice sites. Finally, we would like to mention that Fig. 1 shows how the relative importance of the inhomogeneity decreases as the number of particles increases. This implies that the anomalous inhomogeneity should be only important for small systems with a very small number of particles. We note that the invariance of **G** reduces the number of degrees of freedom of the system (see, e.g., Eq. (10)) and thus it gives rise to a $1/N$ finite-size effect.

The preceding observations can be made clearer by comparing the simulation results of Fig. 1 with the theoretical predictions for the density profile obtained from Eq. (13). For simplicity we shall restrict our attention to the cases $N = 2$ and 3, for which Eq. (13) can be evaluated in a rather direct way.

For $N = 2$ disks of equal mass there are only four CM positions $\mathbf{R}_{0,0}$, $\mathbf{R}_{1,0}$, $\mathbf{R}_{0,1}$, and $\mathbf{R}_{1,1}$. The integrations over $\mathbf{r}_1$ and $\mathbf{r}_2$ can be carried out taking into account the geometry functions $H(\mathbf{r}_i)$ and the integration properties of the δ functions present in Eq. (13) (note that $\hat{\rho}(\mathbf{r})$ is also a sum of δ terms [see Eq. (12)]). After some calculations one obtains:

$$\rho_{{\rm pbc},N=2}(\mathbf{r}) = \rho_0 H(\mathbf{r}) \left(1 + \sum_{\alpha,\beta=0}^{1} f(|2\mathbf{R}_{\alpha,\beta} - 2\mathbf{r}|_{\rm pbc}) \right) \tag{15}$$

where $\rho_0 = N / \int \rho_{\rm pbc}(\mathbf{r}) d\mathbf{r}$ is a normalization constant. Therefore, the $N = 2$ result for $\rho_{\rm pbc}(\mathbf{r})$ is a constant function with four *holes* centered at the CM positions $\mathbf{R}_{\alpha,\beta}$. In order to compare with the simulation results of Fig. 1(a) we choose $\mathbf{R}_{0,0} = (0.75\sigma, 0.75\sigma)$ as the initial value of the CM position in a $3\sigma \times 3\sigma$ cell. In this case one has $\mathbf{R}_{1,0} = (2.25\sigma, 0.75\sigma)$, $\mathbf{R}_{0,1} = (0.75\sigma, 2.25\sigma)$, and $\mathbf{R}_{1,1} = (2.25\sigma, 2.25\sigma)$ which when substituted in Eq. (15) yield a result in complete agreement with the simulation data presented in Fig. 1(a).

The theoretical solution for the density profile of $N = 3$ disks requires integrating over $\mathbf{r}_1$, $\mathbf{r}_2$, and $\mathbf{r}_3$. The integrals over $\mathbf{r}_1$ and $\mathbf{r}_2$ can be carried out like in the $N = 2$ case but the remaining integral over $\mathbf{r}_3$ is more involved. Although analytical results can be obtained at moderate mean densities, in this case it is better to resort to numerical integrations. In Fig. 2 we present our results based on Eq. (10) for a system of 3 disks in square boxes ($L_x = L_y = L$) of different sizes. In all cases $\mathbf{R}_{0,0} = (L/6, L/6)$, $\mathbf{R}_{1,0} = (3L/6, L/6)$, etc. As one can observe, the density profile becomes more inhomogeneous as the size of the box decreases (i.e., as the mean density $\rho_{\rm mean}$ increases), more concretely, the inhomogeneity is negligible for $\rho_{\rm mean} \lesssim 0.1$ but already for $\rho_{\rm mean} \sim 0.3$ it becomes very important. In all cases there are nine peaks located at the CM positions $\mathbf{R}_{\alpha,\beta}$ in agreement with the simulation results of Fig. 1(b). In particular, in Fig. 2(b) we have considered the same box size ($L = 3\sigma$) as in Fig. 1(b), and one can observe a perfect agreement between theory and simulation. This agreement is more evident in Fig. 3 where we compare the results of theory [Eq. (10)] and simulation for the situation presented in Figs. 1(b) and 2(b) ($N = 3$, $L = 3\sigma$) at different fixed values of x.

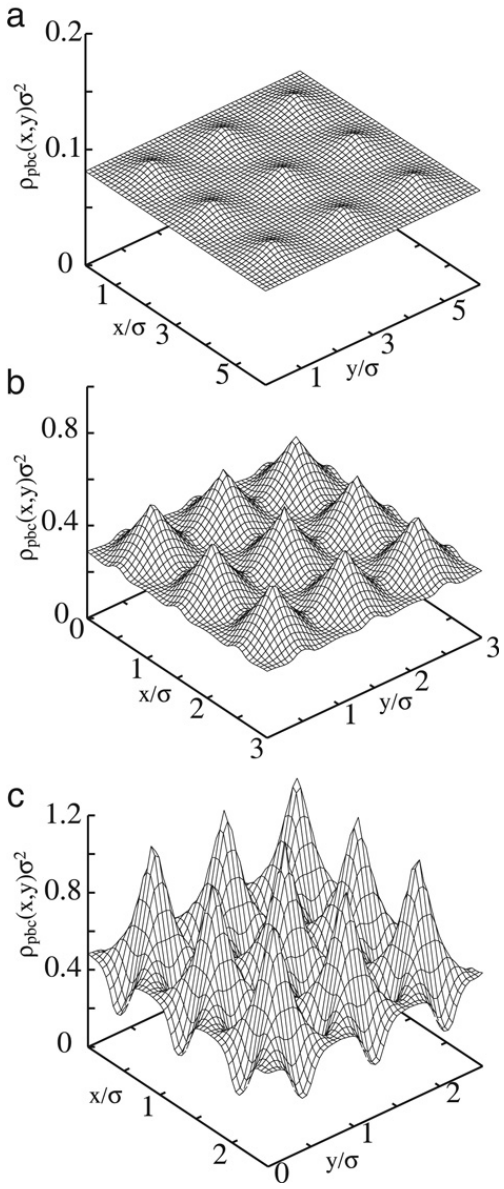

Fig. 2. Theoretical results for the density profile of a hard-disk fluid with periodic boundary conditions and different box sizes. In all cases $N = 3$ and $L_x = L_y = L$; (a) $L = 6\sigma$, (b) $L = 3\sigma$, and (c) $L = 2.5\sigma$. Note the different vertical scales.

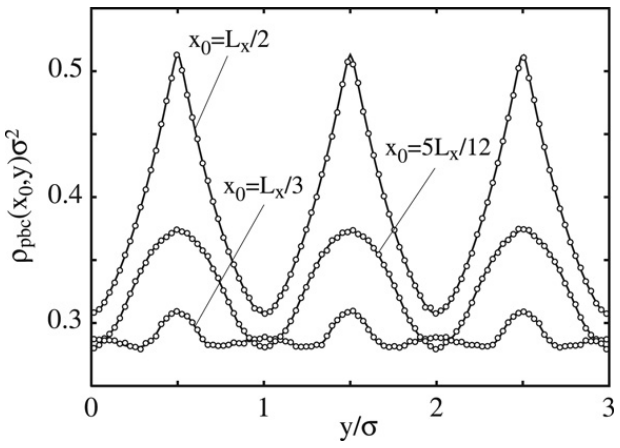

Fig. 3. Density profile of a hard-disk fluid with periodic boundary conditions at different fixed values of x. $N = 3$ and $L_x = L_y = 3\sigma$. The solid lines are the results of Eq. (10). The symbols are simulation data.

In summary, Figs. 1 and 2 show the general behavior of the anomalous inhomogeneity due to the use of periodic boundary conditions: (i) The inhomogeneity decreases with increasing size of the system, being only relevant for very small systems, and (ii) the inhomogeneity increases with increasing mean density, as is usual for inhomogeneous systems.

4. Summary

In this paper we have studied the effect of the invariance of **G** and the CM position in the analysis of *EVN***MG** ensemble averages of quantities that only depend on the spatial coordinate **r**. Two main theoretical expressions have been obtained depending on the coordinates of the system. Eq. (8) yields $\langle A(\mathbf{r})\rangle$ for *infinite-checkerboard* positions while Eq. (10) is our result for simulation-cell positions used in MD simulations. In the latter case, instead of one CM position one has to deal with a distribution of CM positions. For a system consisting of N hard disks of equal mass there are N^2 CM positions $\mathbf{R}_{\alpha,\beta}$ distributed in a rectangular (square) sublattice. It is precisely the geometry of this sublattice that determines the structure of the fluid as one can see both in simulation and in theory results.

As an example we have found an anomalous inhomogeneity in the MD result for the density profile of an isolated system of hard disks without external forces due to the consideration of periodic boundary conditions. We note that under these circumstances, the total linear momentum **M** of the system and the generator of infinitesimal Galilean boosts **G** are invariants of the equations of motion of the system and one has to work in the context of the *EVN***MG** ensemble.

Of course, the anomalous inhomogeneity in the density profile can only be observed for systems with a very small number of particles ($N \lesssim 10$) for which the number of CM positions (N^2) is relatively small. In fact, for larger systems the differences among the *EVN*, the *EVN***M** and the *EVN***MG** ensembles are of order $1/N$ (see Ref. [9]) and we expect little impact of this inhomogeneity that should decrease with increasing size of the system. This trend can already be observed in Fig. 1. One can see that as N increases the inhomogeneity becomes smoother. In any case, when performing a MD simulation of a system with N small one should be aware of this anomalous behavior that could affect the measurement of basic quantities like the pair correlation function of the system or even modify the nature of the freezing transition due to the appearance of pinning sites associated with the anomalous inhomogeneity. In addition, since the position of the CM distribution depends on the initial value of **R** one reaches the intriguing conclusion that the structure of the density profile depends on the initial conditions of the system.

Finally, we would like to remark that a system with disks with irrational mass ratios gives rise to a continuum distribution of CM which washes out the structure of the density profile and its influence on related quantities like the pair correlation function.

Acknowledgment

This work was supported by *Ministerio de Educación y Ciencia* of Spain under Grants FIS2005-05081 FEDER and FIS2006-03764 FEDER.

References

[1] J.L. Lebowitz, J.K. Percus, L. Verlet, Phys. Rev. 153 (1967) 250.
[2] W.W. Wood, in: E.G.D. Cohen (Ed.), Fundamental Problems in Statistical Mechanics, Vol. 3, North-Holland, Amsterdam, 1975.
[3] J.J. Erpenbeck, W.W. Wood, in: B.J. Berne (Ed.), Modern Theoretical Chemistry, in: Statistical Mechanics, Part B, vol. 6, Plenum Press, New York, 1977.
[4] F. Lado, J. Chem. Phys. 75 (1981) 5461.
[5] T. Çağin, J.R. Ray, Phys. Rev. A 37 (1988) 247.
[6] T. Çağin, J.R. Ray, Phys. Rev. A 37 (1988) 4510.
[7] F.L. Román, J.A. White, S. Velasco, Phys. Rev. E 51 (1995) 6271.
[8] F.L. Román, A. González, J.A. White, S. Velasco, Physica A 234 (1996) 53.
[9] J.R. Ray, H. Zhang, Phys. Rev. E 59 (1999) 4781.
[10] W.W. Wood, J.J. Erpenbeck, G.A. Baker Jr., J.D. Johnson, Phys. Rev. E 63 (2000) 011106.
[11] R.B. Shirts, S.R. Burt, A.M. Johnson, J. Chem. Phys. 125 (2006) 164102. For related work see also;
M.J. Uline, D.W. Siderius, D.S. Corti, J. Chem. Phys. 128 (2008) 124301;
L.A. Openov, A.I. Podlivaev, Phys. Solid State 50 (2008) 1195.
[12] J.L. Lebowitz, J.K. Percus, Phys. Rev. 124 (1961) 1673.
[13] L.R. Pratt, S.W. Haan, J. Chem. Phys. 74 (1981) 1864; J. Chem. Phys. 74 (1981) 1873.
[14] A.R. Denton, P.A. Egelstaff, Z. Phys. B 103 (1997) 343.
[15] F.L. Román, J.A. White, A. González, S. Velasco, J. Chem. Phys. 110 (1999) 9821.
[16] E.M. Pearson, T. Halicioglu, W.A. Tiller, Phys. Rev. A 32 (1985) 3030.
[17] D.C. Rapaport, The Art of Molecular Dynamics Simulation, Cambridge University Press, Cambridge, 1997.